NMR studies on intramolecular mobility of *ortho*-substituted push-pull phenyl butadienes †

Thomas Freier,[a] Manfred Michalik,*[a] Klaus Peseke[b] and Helmut Reinke[b]

[a] *Institut für Organische Katalyseforschung an der Universität Rostock e.V., Buchbinderstr. 5–6, D-18055 Rostock, Germany*
[b] *Fachbereich Chemie der Universität Rostock, Buchbinderstr. 7, D-18055 Rostock, Germany*

Received (in Cambridge) 27th July 1998, Accepted 30th March 1999

The ^{1}H and ^{13}C NMR spectra of a series of 3-aryl-2-cyano-5,5-bis(methylthio)penta-2,4-dienenitriles (**3**) and 3-aryl-2-cyano-5-dimethylamino-5-methylthiopenta-2,4-dienenitriles (**4**) with different *ortho*-phenyl substituents were recorded. The NMR data are compared with those of the corresponding *para*-substituted compounds **1** and **2**. Dynamic ^{1}H NMR measurements showed rotation processes about the C-2,C-3, C-3,C-4, C-4,C-5, and C-5,N bonds. The free energies of activation $\Delta G_c^{\ddagger}$ are discussed with respect to electronic and steric effects of the substituents. The magnitude of the rotation barriers correlates with the variation in bond lengths and angles as determined by X-ray structure analyses.

Introduction

Push-pull butadienes (butadienes of type **I** with donor groups D and acceptor groups A at the terminal carbon atoms, Scheme 1) are characterized by significant π-electron interactions

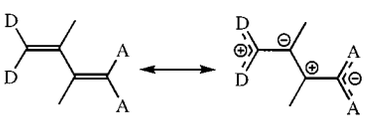

Ia **Ib**

Scheme 1

between the donor and acceptor groups and the diene double bond system. The push-pull substitution alters the polyene state of the unsubstituted butadiene with balanced π-charge distribution to a polymethine structure[2] with alternating charge densities at the C-atoms. This is reflected in the ^{13}C NMR chemical shifts of the substituted butadienes.[1,3–7]

Furthermore, the charge redistribution in the butadiene chain leads to a decrease in the barrier to rotation about the double bonds and to an increase in the barrier to rotation about the single bonds. As a consequence, these processes come into the NMR timescale and can be observed by dynamic NMR spectroscopy.[1,4,6,8–10]

In our studies on stereochemistry and intramolecular mobility of the *para*-phenyl substituted butadiene derivatives **1** and **2** (Scheme 2) we observed slow rotations about the C-2,C-3, C-3, C-4, C-4,C-5, and C-5,N (in **2**) bonds.[1,9] Whereas the barriers to rotation about C,C double bonds in simple ethenes are typically above 250 kJ mol^{-1},[11] the energy barrier of the C-4,C-5 bond in **1** is decreased to about 90 kJ mol^{-1}.[9] Substitution of one methylthio by a dimethylamino group in **2** leads to a further decrease to about 30 kJ mol^{-1}.[1] The reason for this effect is the stronger donor capacity of the amino group which leads to greater single-bond character of the formal C-4,C-5 double bond.

In the case of single bonds the rotation barriers are normally less than 15 kJ mol^{-1}.[12] However, in compounds **2** the values are about 40 kJ mol^{-1} thus the C-3,C-4 and C-5,N rotations are

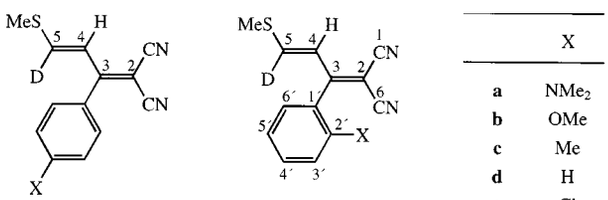

1 (D = MeS)
2 (D = Me_2N)

3 (D = MeS)
4 (D = Me_2N)

	X
a	NMe_2
b	OMe
c	Me
d	H
e	Cl
f	Br
g	NO_2
h	*i*-Pr

Scheme 2

observed in the low-temperature spectra.[1] Significantly, these barriers are higher than those observed for the C-4,C-5 double bond. A further increase of the C-3,C-4 rotation barrier to about 70 kJ mol^{-1} is established for bis(dimethylamino)-substituted butadienes.[13]

^{1}H NMR studies[1,14] and X-ray structure analyses[15,16] show that the phenyl ring in **1** and **2** is twisted out of the plane of the butadiene system due to steric interactions with the donor and acceptor groups. Referring to this fact we introduced a substituent into the *ortho*-position of the phenyl ring to attain axially-chiral push-pull butadienes **3** and **4** (Scheme 2) as precursors for asymmetric syntheses of chiral heterocycles. However, the chirality axis in **3** and **4** proved to be dynamic at room temperature.[17]

As in the case of *para*-substituted compounds **1** and **2** we also found significant lineshape alterations in the ^{1}H NMR spectra for **3** and **4** which can be assigned to different dynamic processes about the butadiene bonds. These investigations are the subject of the present paper. For example, the ^{1}H and ^{13}C chemical shifts and dynamic NMR parameters of the *ortho*-substituted compounds are compared in terms of electronic and steric factors to the *para*-substituted compounds.

Experimental

The ^{1}H and ^{13}C NMR measurements on 0.05 M solutions of **3** and **4** were performed on a Bruker ARX-300 spectrometer at 300.1 MHz and 75.5 MHz, respectively. In addition, a solution of **4c** in CD_2Cl_2–$CHCl_2F$ (1 : 4) was also measured at low temperatures with a Bruker ARX-400 spectrometer at 400.1 MHz.

† Spectroscopic investigations on butadiene derivatives, Part 9. For Part 8, see Ref. 1.

Table 1 ^{1}H and ^{13}C chemical shifts δ (ppm, TMS = 0 ppm) of compounds **3** in $CDCl_3$ at 303 K

	3a	**3b**	**3c**	**3d**	**3e**	**3f**	**3g**	**3h**
H-4	6.56	6.55	6.56	6.51	6.57	6.56	6.60	6.58
SCH_3	2.60d[a]	2.58	2.60	2.59	2.61	2.61	2.61	2.61
SCH_3	2.33	2.30	2.31	2.28	2.34	2.35	2.30	2.31
other signals	[b]	[c]	[d]	[e]	[f]	[g]	[h]	[i]
C-2	77.1	78.6	77.2	78.1	78.3	78.2	77.5	77.6
C-3	167.4	164.7	167.2	167.9	163.9	165.2	164.2	167.5
C-4	113.5	113.9	112.3	114.1	112.6	112.5	112.7	112.8
C-5	163.0	163.9	166.1	164.9	166.0	166.1	165.2	166.1
CN	114.7	114.4	114.1	114.3	113.8	113.8	113.6	114.3
CN	114.7	114.1	114.0	114.0	113.6	113.7	113.3	114.0
SCH_3	17.6	17.6	17.7	17.7	17.7	17.8	17.7	17.7
SCH_3	16.5	16.4	16.3	16.7	16.5	16.6	16.6	16.2
other signals	[j]	[k]	[l]	[m]	[n]	[o]	[p]	[q]

[a] J = 0.5 Hz. [b] 2.79 (s, 6H, NCH_3), 7.01 (m, 1H, H-3′), 7.36 (m, 1H, H-4′), 6.94 (m, 1H, H-5′), 7.01 (m, 1H, H-6′). [c] 3.86 (s, 3H, OCH_3), 6.96 (m, 1H, H-3′), 7.44 (m, 1H, H-4′), 7.02 (m, 1H, H-5′), 7.07 (m, 1H, H-6′). [d] 2.23 (s, 3H, CH_3), 7.25 (m, 1H, H-3′), 7.37 (m, 1H, H-4′), 7.27 (m, 1H, H-5′), 7.05 (m, 1H, H-6′). [e] 7.32–7.36 (m, 2H, H-3′, 5′), 7.42–7.54 (m, 3H, H-2′, 4′, 6′). [f] 7.47 (m, 1H, H-3′), 7.43 (m, 1H, H-4′), 7.36 (m, 1H, H-5′), 7.20 (m, 1H, H-6′). [g] 7.64 (m, 1H, H-3′), 7.34 (m, 1H, H-4′), 7.42 (m, 1H, H-5′), 7.19 (m, 1H, H-6′). [h] 8.27 (m, 1H, H-3′), 7.69 (m, 1H, H-4′), 7.77 (m, 1H, H-5′), 7.34 (m, 1H, H-6′). [i] 1.23 (d, 3H, $CHCH_3$, J = 6.8 Hz), 1.25 (d, 3H, $CHCH_3$, J = 6.8 Hz), 2.77 (m, 1H, $CHCH_3$), 7.38 (m, 1H, H-3′), 7.45 (m, 1H, H-4′), 7.26 (m, 1H, H-5′), 7.01 (m, 1H, H-6′). [j] 43.2 (NCH_3), 125.8 (C-1′), 151.6 (C-2′), 118.7 (C-3′), 132.0 (C-4′), 121.1 (C-5′), 130.3 (C-6′). [k] 55.9 (OCH_3), 123.8 (C-1′), 156.5 (C-2′), 111.8 (C-3′), 132.4 (C-4′), 121.3 (C-5′), 129.5 (C-6′). [l] 19.3 (CH_3), 134.4 (C-1′), 135.6 (C-2′), 131.0 (C-3′), 130.6 (C-4′), 126.8 (C-5′), 127.7 (C-6′). [m] 134.6 (C-1′), 128.6 (C-2′, 6′), 129.1 (C-3′, 5′), 131.2 (C-4′). [n] 133.9 (C-1′), 132.6 (C-2′), 130.4 (C-3′), 131.8 (C-4′), 127.7 (C-5′), 129.6 (C-6′). [o] 135.9 (C-1′), 122.0 (C-2′), 133.5 (C-3′), 131.8 (C-4′), 128.3 (C-5′), 129.6 (C-6′). [p] 130.8 (C-1′), 147.2 (C-2′), 125.9 (C-3′), 131.7 (C-4′), 134.7 (C-5′), 130.5 (C-6′). [q] 23.1 ($CHCH_3$), 24.6 ($CHCH_3$), 31.0 ($CHCH_3$), 133.3 (C-1′), 146.1 (C-2′), 126.5 (C-3′), 130.9 (C-4′), 126.8 (C-5′), 127.6 (C-6′).

Table 2 ^{1}H and ^{13}C chemical shifts δ (ppm, TMS = 0 ppm) of compounds **4** in $CDCl_3$ at 303 K

	4a	**4b**	**4c**	**4d**	**4e**	**4f**	**4g**	**4h**
H-4	5.57	5.56	5.71	5.35	5.67	5.68	5.69	5.67
SCH_3	2.18	2.19	2.02	2.29	2.09	2.08	1.99	2.05
NCH_3	3.03	3.06	3.15	3.06	3.21	3.22	3.20	3.21
other signals	[a]	[b]	[c]	[d]	[e]	[f]	[g]	[h]
C-2	64.5	65.9	67.3	62.7	66.7	67.0	67.0	67.4
C-3	168.9	166.2	169.8	168.8	165.9	167.4	165.6	169.7
C-4	98.2	99.8	101.4	97.9	100.9	101.2	101.2	101.9
C-5	170.7	170.3	168.4	172.6	169.0	168.4	167.2	168.6
CN	117.6	117.3	116.6	117.6	116.4	116.3	116.0	116.5
CN	117.5	117.1	116.5	117.4	116.4	116.3	115.8	116.4
SCH_3	18.1	18.1	17.9	18.4	18.2	18.2	18.3	18.2
NCH_3	42.9	42.9	42.7	43.2	42.8	42.8	42.6	42.7
other signals	[i]	[j]	[k]	[l]	[m]	[n]	[o]	[p]

[a] 2.74 (s, 6H, NCH_3), 6.95 (m, 1H, H-3′), 7.29 (m, 1H, H-4′), 6.94 (m, 1H, H-5′), 7.13 (m, 1H, H-6′). [b] 3.84 (s, 3H, OCH_3), 6.93 (m, 1H, H-3′), 7.36 (m, 1H, H-4′), 6.95 (m, 1H, H-5′), 7.09 (m, 1H, H-6′). [c] 2.30 (s, 3H, CH_3), 7.20 (m, 1H, H-3′), 7.27 (m, 1H, H-4′), 7.17 (m, 1H, H-5′), 7.05 (m, 1H, H-6′). [d] 7.38–7.45 (m, 5H, H-2′-6′). [e] 7.41 (m, 1H, H-3′), 7.33 (m, 1H, H-4′), 7.30 (m, 1H, H-5′), 7.26 (m, 1H, H-6′). [f] 7.59 (m, 1H, H-3′), 7.24 (m, 1H, H-4′), 7.35 (m, 1H, H-5′), 7.25 (m, 1H, H-6′). [g] 8.04 (m, 1H, H-3′), 7.57 (m, 1H, H-4′), 7.67 (m, 1H, H-5′), 7.41 (m, 1H, H-6′). [h] 1.17 (d, 3H, $CHCH_3$, J = 6.9 Hz), 1.28 (d, 3H, $CHCH_3$, J = 6.8 Hz), 2.97 (m, 1H, $CHCH_3$), 7.32–7.38 (m, 2H, H-3′, 4′), 7.18 (m, 1H, H-5′), 7.04 (m, 1H, H-6′). [i] 43.3 (NCH_3), 128.8 (C-1′), 151.3 (C-2′), 117.8 (C-3′), 130.8 (C-4′), 120.8 (C-5′), 131.0 (C-6′). [j] 55.6 (OCH_3), 126.5 (C-1′), 156.7 (C-2′), 111.4 (C-3′), 131.3 (C-4′), 120.4 (C-5′), 129.9 (C-6′). [k] 19.7 (CH_3), 137.3 (C-1′), 135.9 (C-2′), 130.5 (C-3′), 129.3 (C-4′), 125.6 (C-5′), 128.3 (C-6′). [l] 137.2 (C-1′), 129.2 (C-2′, 6′), 128.4 (C-3′, 5′), 130.7 (C-4′). [m] 136.5 (C-1′), 132.5 (C-2′), 130.0 (C-3′), 130.5 (C-4′), 126.8 (C-5′), 130.5 (C-6′). [n] 138.5 (C-1′), 122.2 (C-2′), 133.1 (C-3′), 130.5, 130.6 (C-4′, 6′), 127.3 (C-5′). [o] 133.1 (C-1′), 148.3 (C-2′), 124.7 (C-3′), 130.4 (C-4′), 133.2 (C-5′), 131.1 (C-6′). [p] 24.0 ($CHCH_3$), 24.3 ($CHCH_3$), 30.4 ($CHCH_3$), 136.3 (C-1′), 145.9 (C-2′), 125.9 (C-3′), 129.6 (C-4′), 125.5 (C-5′), 128.2 (C-6′).

Solvents given in Tables 1–4 were dried over molecular sieves or sodium sulfate, the halogen containing solvents were purified with basic aluminium oxide to remove acid impurities.

For low-temperature measurements, argon was bubbled through the solution to remove impurities of paramagnetic oxygen. The probe temperature was measured by means of thermometer liquids.[18] The exchange rates at the coalescence point were obtained in the case of equally populated sites using the Gutowsky–Holm relationship,[19] and for unequal populations using the equations of Shanan-Atidi and Bar-Eli.[20] The free energies of activation were calculated from the Eyring equation. The error limits were estimated to be $T_c = \pm 2$ K, $\Delta\nu_c = \pm 10\%$, $p_c = \pm 0.05$, and $\Delta G^{\ddagger}_c = \pm 0.8$ kJ mol^{-1}.

The X-ray diffraction results were obtained on a Siemens P4 four circle diffractometer with λ(Mo-Kα) = 0.71073 Å. After taking rotational photos and determining reasonable reduced cells a data collection was started in routine ω-scan. The structures were solved with direct methods (SHELXTL, Siemens Analytical X-ray Instruments Inc.) and refined with the full-matrix least-squares method of SHELXL-93.[21] All non-hydrogen atoms were refined anisotropically whereas the hydrogens were put into theoretical positions and refined according to the riding model.

Compounds **5** were prepared according to the procedures for Knoevenagel reactions.[22] The bis(methylthio)butadienes **3** were prepared by reaction of the Knoevenagel products **5** with carbon disulfide and methyl iodide in the presence of sodium hydride (Scheme 3).[1] Treatment of **3** with aqueous dimethylamine gave the amino compounds **4**.[23]

For all compounds, the experimental values of elemental analysis correspond to the calculated values within acceptable limits (±0.5).

Preparation of 3 according to ref. 1

In an inert gas atmosphere, 0.01 mol of **5**, 1.52 g (0.02 mol)

Table 3 Dynamic NMR parameters (300 MHz), free energies of activation and differences $\Delta\Delta G_c^{\ddagger} = \Delta G_c^{\ddagger}(\mathbf{3}) - \Delta G_c^{\ddagger}(\mathbf{1})$ for the restricted rotation about the C-4, C-5 bond in the butadienes **1** and **3** (solvent DMSO-d_6, obsd. signal SMe)

	1			**3**			
	T_c/K	$\Delta\nu_c$/Hz	$\Delta G_c^{\ddagger}$/kJ mol^{-1}	T_c/K	$\Delta\nu_c$/Hz	$\Delta G_c^{\ddagger}$/kJ mol^{-1}	$\Delta\Delta G_c^{\ddagger}$/kJ mol^{-1}
a	458[a]	70[a]	96.5[a]	447	83	91.5	−5.0
b	436	86	89.0	439	92	89.3	0.3
c	431	93	87.7	436	95	88.7	1.0
d	427	99	86.6	427	99	86.6	0
e	418	92	85.0	423	89	86.1	1.1
f	418	92	85.0	425	88	86.6	1.6
g	397	104	80.1	421	101	85.2	5.1
h	434	94	88.4	442	93	89.9	1.5

[a] The coalescence point of **1a** was above the available range of measurement. $\Delta G^{\ddagger}$ was measured at 458 K by the intensity method[29] to be 96.5 kJ mol^{-1}.

Table 4 Dynamic NMR parameters (300 MHz), free energies of activation and differences $\Delta\Delta G_c^{\ddagger} = \Delta G_c^{\ddagger}(\mathbf{4}) - \Delta G_c^{\ddagger}(\mathbf{2})$[1] for the restricted rotations in the butadienes **4** (0.05 M in CD_2Cl_2)

4	Obsd. signal	T_c/K	$\Delta\nu_c$/Hz	p_c	$\Delta G_c^{\ddagger}$/kJ mol^{-1}	$\Delta\Delta G_c^{\ddagger}$/kJ mol^{-1}
Rotation about the C-3,C-4 bond[a]						
a	H-4	210	175	0.95	45.5; 40.4	8.9; 4.9
b	SMe	196	80	0.89[b]	42.3; 38.9	2.2; 0.0
c	SMe	207	175	0.90[b]	43.6; 39.8	2.7; 0.2
d	H-4	211	229	0.68	41.7; 40.4	0; 0
e	SMe	214	180	0.90[b]	45.2; 41.3	2.8; 0.4
f	SMe	215	180	0.90[b]	45.3; 41.4	2.6; 0.3
g	SMe	212	195	0.92[b]	45.0; 40.7	1.2; −1.3
Rotation about the C-4,C-5 bond, s-cis compounds[c]						
a[d]	H-4	186	90 ± 15	0.75	38.5; 36.8	3.9; 3.3
b	SMe	185	10	0.69[b]	41.2; 39.9	—
c	SMe	198	15	0.34[b]	42.2; 43.3	—
c[d,e]	SMe	162	62	0.18	32.3; 34.3	—
e	SMe	197	15	0.76	43.7; 41.8	—
f	SMe	207	24	0.67	44.5; 43.3	—
g	SMe	204	19	0.86	44.4; 41.3	—
Rotation about the C-5,N bond, s-cis compounds[f]						
a	NMe_2	208	135	—	40.4	4.7[g]
b	NMe_2	202	89	—	39.8	0.8
c	NMe_2	208	98	—	40.9	1.0
d	NMe_2	210	133	—	40.9	0
e	NMe_2	210	64	—	42.1	0.8
f	NMe_2	207	47	—	42.1	0.7
g	NMe_2	204	68	—	40.8	−1.6

[a] p_c of s-*trans* compound. [b] p_c (determd. on signal H-4). [c] Assignment of *E*/*Z* impossible; p_c of low-field signal of the H-4 signals belonging to s-*cis* conformer. [d] s-*trans* compound, p_c of *E* compound. [e] In CD_2Cl_2–$CHCl_2F$ (1 : 4) (400 MHz). [f] $\Delta G_c^{\ddagger}$ and $\Delta\Delta G_c^{\ddagger}$ represent lower limits (see text). [g] $\Delta G_c^{\ddagger}$ of **2a** calculated (see text).

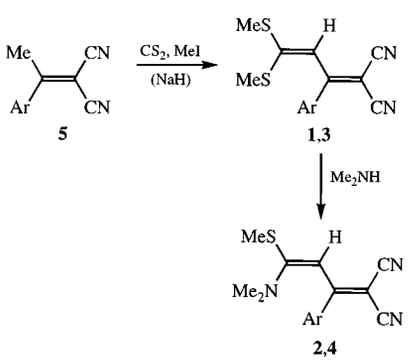

Scheme 3

carbon disulfide and 7.10 g (0.05 mol) methyl iodide in 50 ml absolute dimethylformamide were added, with stirring, to 0.60 g (0.025 mol) sodium hydride. After stirring for 1 h the reaction mixture was placed in 200 ml ice–water and left to stand for several days to crystallize. The precipitate was separated, washed with water and light petroleum and recrystallized from ethanol or acetic acid.

2-Cyano-3-(2-dimethylaminophenyl)-5,5-bis(methylthio)-penta-2,4-dienenitrile (3a). Yield: 2.20 g (64%), violet crystals, mp 135–136 °C (EtOH). NMR: see Table 1. MS (70 eV): *m*/*z* = 315 (M^+). IR (KBr): $\tilde{\nu}$ = 2211 cm^{-1} (CN), 2202 cm^{-1} (CN). UV (EtOH): λ_{max} (log ε) = 264 nm (3.99), 296 nm (3.91), 403.5 nm (4.37).

2-Cyano-3-(2-methoxyphenyl)-5,5-bis(methylthio)penta-2,4-dienenitrile (3b). Yield: 2.42 g (80%), yellow crystals, mp 142–143 °C (EtOH). NMR: see Table 1. MS (70 eV): *m*/*z* = 302 (M^+). IR (KBr): $\tilde{\nu}$ = 2210 cm^{-1} (CN). UV (EtOH): λ_{max} (log ε) = 256.5 nm (3.90), 303.5 nm (3.80), 410.5 nm (4.36).

2-Cyano-3-(2-methylphenyl)-5,5-bis(methylthio)penta-2,4-dienenitrile (3c). Yield: 2.31 g (81%), yellow crystals, mp 118–120 °C (EtOH). NMR: see Table 1. MS (70 eV): *m*/*z* = 286 (M^+). IR (KBr): $\tilde{\nu}$ = 2211 cm^{-1} (CN). UV (EtOH): λ_{max} (log ε) = 262 nm (3.46), 310 nm (3.78), 412 nm (4.47).

3-(2-Chlorophenyl)-2-cyano-5,5-bis(methylthio)penta-2,4-dienenitrile (3e). Yield: 1.97 g (64%), yellow and violet crystals, mp 102 °C (EtOH). NMR: see Table 1. MS (70 eV): m/z = 306 (M^+). IR (KBr): $\tilde{\nu}$ = 2213 cm^{-1} (CN). UV (EtOH): λ_{max} (log ε) = 310 nm (3.75), 414 nm (4.45).

3-(2-Bromophenyl)-2-cyano-5,5-bis(methylthio)penta-2,4-dienenitrile (3f). Yield: 2.57 g (73%), yellow and violet crystals, mp 101 °C (EtOH). NMR: see Table 1. MS (70 eV): m/z = 350 (M^+). IR (KBr): $\tilde{\nu}$ = 2212 cm^{-1} (CN). UV (EtOH): λ_{max} (log ε) = 310 nm (3.77), 414.5 nm (4.46).

2-Cyano-5,5-bis(methylthio)-3-(2-nitrophenyl)penta-2,4-dienenitrile (3g). Yield: 2.62 g (83%), yellow and violet crystals, mp 171–173 °C (MeCOOH). NMR: see Table 1. MS (70 eV): m/z = 317 (M^+). IR (KBr): $\tilde{\nu}$ = 2217 cm^{-1} (CN). UV (EtOH): λ_{max} (log ε) = 273 nm (3.75), 305.5 nm (3.69), 412 nm (4.36).

2-Cyano-3-(2-isopropylphenyl)-5,5-bis(methylthio)penta-2,4-dienenitrile (3h). Yield: 2.57 g (82%), yellow crystals, mp 88–89 °C (EtOH). NMR: see Table 1. MS (70 eV): m/z = 314 (M^+). IR (KBr): $\tilde{\nu}$ = 2213 cm^{-1} (CN). UV (EtOH): λ_{max} (log ε) = 258.5 nm (3.45), 314 nm (3.72), 413 nm (4.43).

Preparation of 4 according to ref. 1

2 ml of 40% aqueous dimethylamine solution were added dropwise over two hours to a solution of 2 mmol of **3** in 8 ml THF at reflux temperature. After another hour the reaction progress was determined by TLC (SiO_2/CH_2Cl_2) and, if necessary, further dimethylamine solution was added. Upon completion, the THF was distilled off, the residue dissolved in 20 ml chloroform, washed with water and dried over sodium sulfate. Then, the solvent was removed and the substance recrystallized from ethanol.

2-Cyano-5-dimethylamino-3-(2-dimethylaminophenyl)-5-methylthiopenta-2,4-dienenitrile (4a). Yield: 0.31 g (50%), orange crystals, mp 121–123 °C (EtOH). NMR: see Table 2. MS (70 eV): m/z = 312 (M^+). IR (KBr): $\tilde{\nu}$ = 2195 cm^{-1} (CN), 2181 cm^{-1} (CN). UV (EtOH): λ_{max} (log ε) = 266.5 nm (4.14), 429.5 nm (4.37).

2-Cyano-5-dimethylamino-3-(2-methoxyphenyl)-5-methylthiopenta-2,4-dienenitrile (4b). Yield: 0.42 g (70%), orange crystals, mp 147–150 °C (EtOH). NMR: see Table 2. MS (70 eV): m/z = 299 (M^+). IR (KBr): $\tilde{\nu}$ = 2200 cm^{-1} (CN), 2185 cm^{-1} (CN). UV (EtOH): λ_{max} (log ε) = 261.5 nm (3.91), 429.5 nm (4.49).

2-Cyano-5-dimethylamino-3-(2-methylphenyl)-5-methylthiopenta-2,4-dienenitrile (4c). Yield: 0.41 g (72%), red crystals, mp 163 °C (EtOH). NMR: see Table 2. MS (70 eV): m/z = 283 (M^+). IR (KBr): $\tilde{\nu}$ = 2193 cm^{-1} (CN), 2162 cm^{-1} (CN). UV (EtOH): λ_{max} (log ε) = 273.5 nm (3.85), 423.5 nm (4.55).

3-(2-Chlorophenyl)-2-cyano-5-dimethylamino-5-methylthiopenta-2,4-dienenitrile (4e). Yield: 0.43 g (71%), orange crystals, mp 148–150 °C (EtOH). NMR: see Table 2. MS (70 eV): m/z = 303 (M^+). IR (KBr): $\tilde{\nu}$ = 2193 cm^{-1} (CN), 2162 cm^{-1} (CN). UV (EtOH): λ_{max} (log ε) = 272.5 nm (3.84), 426.5 nm (4.51).

3-(2-Bromophenyl)-2-cyano-5-dimethylamino-5-methylthiopenta-2,4-dienenitrile (4f). Yield: 0.57 g (82%), orange crystals, mp 158–160 °C (EtOH). NMR: see Table 2. MS (70 eV): m/z = 349 + 347 (M^+). IR (KBr): $\tilde{\nu}$ = 2193 cm^{-1} (CN), 2160 cm^{-1} (CN). UV (EtOH): λ_{max} (log ε) = 273 nm (3.85), 427 nm (4.53).

2-Cyano-5-dimethylamino-5-methylthio-3-(2-nitrophenyl)-penta-2,4-dienenitrile (4g). Yield: 0.47 g (75%), orange crystals, mp 155–156 °C (EtOH). NMR: see Table 2. MS (70 eV): m/z = 314 (M^+). IR (KBr): $\tilde{\nu}$ = 2200 cm^{-1} (CN), 2193 cm^{-1} (CN). UV (EtOH): λ_{max} (log ε) = 426 nm (4.42).

2-Cyano-5-dimethylamino-3-(2-isopropylphenyl)-5-methylthiopenta-2,4-dienenitrile (4h). Setting up: 1 mmol **3h**, yield: 0.19 g (61%), yellow crystals, mp 126–127 °C (EtOH). NMR: see Table 2. MS (70 eV): m/z 311 (M^+). IR (KBr): $\tilde{\nu}$ = 2203 cm^{-1} (CN), 2195 cm^{-1} (CN). UV (EtOH): λ_{max} (log ε) = 270.5 nm (3.79), 424 nm (4.53).

Results and discussion

^1H and ^{13}C NMR chemical shifts

The ^1H and ^{13}C chemical shifts of compounds **3** and **4** are summarized in Tables 1 and 2. The chemical shifts of H-4 and C-2 to C-5 are well suited for spectroscopic comparisons.

Linear correlations between the chemical shifts and substituent constants as were found for the *para*-substituted compounds **1** and **2**[1,6,9] could not be confirmed for the *ortho*-compounds **3** and **4** due to competing electronic and steric interactions. The low-field shifts of the H-4 signal for **3** and **4** compared to **1** and **2** can be attributed to the preference of the s-*trans* conformation in the *ortho*-compounds. By low-temperature NMR measurements a population of 90% s-*trans* was found for **4** (Table 4) compared to 70% s-*trans* for **2**[1] at 200 K (see below).

The polymethine character, which is indicated by the alternating shifts of the atoms C-2 to C-5 in such compounds,[4,6] is also confirmed for **3** and **4**. The same is true for the increase of push-pull character of the butadienes by substitution of one SMe group of **3** (Table 1) by an NMe_2 group giving **4** (Table 2) as can be seen from the corresponding signal shifts of C-2 and C-4 to higher and C-3 and C-5 to lower field.[6] These results can be explained by an increased weight of the structure **Ib** (Scheme 1). Generally, the differences in the ^{13}C chemical shifts between *ortho*- and *para*-substituted compounds are relatively small and, therefore, not representative of conformational or electronic changes in the compounds studied.

Dynamic NMR results

The rotations about C-3,C-4, C-4,C-5, and C-5,N bonds are detectable in the ^1H NMR spectra. In the case of **3** only the symmetrical exchange of the two methylthio groups is observed; this is assigned to the C-4,C-5 rotation.[9]

For compounds **4**, the analysis is more complicated since rotation about all three bonds occurs. The assignments were made on the basis of population ratios and signal separations due to the anisotropy effect of the phenyl ring, which is twisted out of the butadiene plane (Scheme 4).[1] The splitting patterns of signals in the ^1H NMR spectra of all compounds **4** are similar. The observed lineshape changes are shown in Figs. 1 and 2 for **4c** measured at 300 and 400 MHz, respectively.

In the 300 MHz spectrum of **4c** in CD_2Cl_2, on cooling below 208 K, the H-4 signal is split into two signals with the intensity ratio of 0.90 (low-field signal) : 0.10 (rotation about C-3,C-4 bond). On further cooling, the high-field signal (s-*cis* conformer) splits below 195 K (rotation about C-4,C-5 bond). The intensity ratio of the resulting signals is 0.34 (low-field signal) : 0.66.

The SMe signal decoalesces into two signals with a population ratio of 0.10 (low-field signal) : 0.90 (rotation about C-3,C-4 bond). The low-field signal (s-*cis* conformer) is split at *ca.* 198 K into two signals; the intensities are 0.66 (low-field signal) : 0.34 (rotation about C-4,C-5 bond).

The NMe_2 signal shows broadening and, below 208 K, splits into three signals with the intensity ratio of 0.05 : 0.05 : 0.90 (rotations about C-5,N and C-3,C-4 bonds). The observed doublet of equally intense signals for the s-*cis* conformer is assigned to the symmetrical exchange of the NMe groups

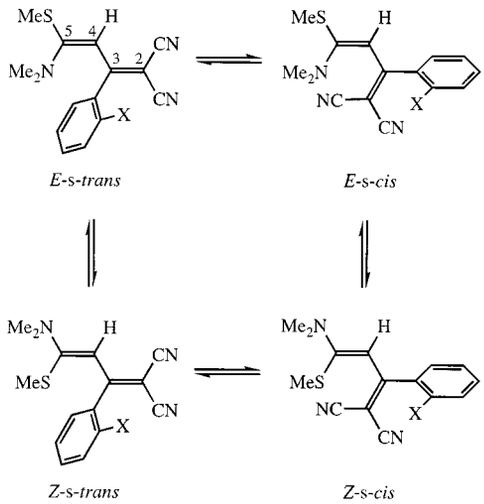

Scheme 4

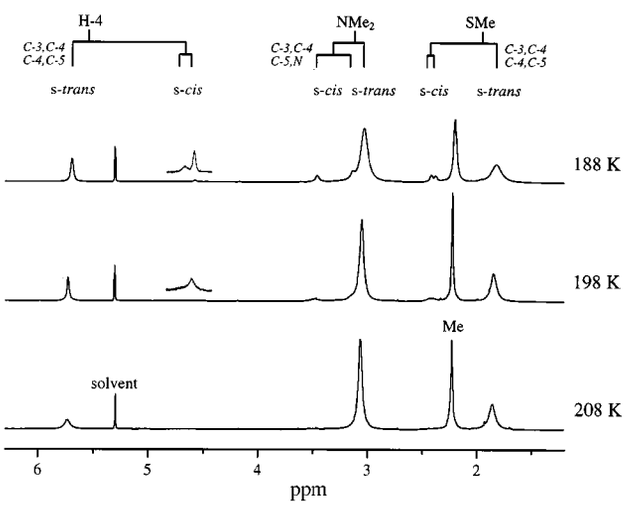

Fig. 1 Temperature-dependent 300 MHz ^{1}H NMR spectra of **4c** in CD_2Cl_2 (208–188 K).

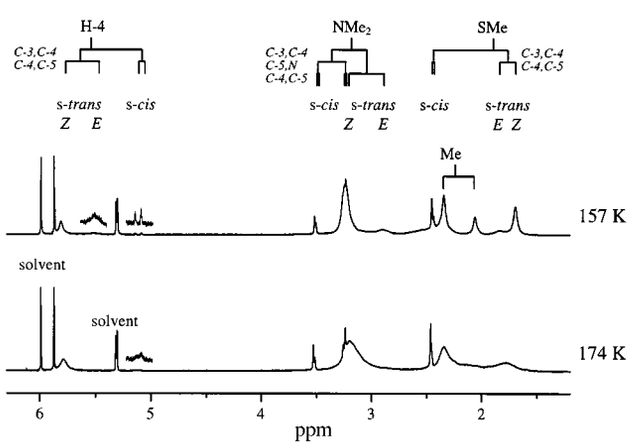

Fig. 2 Temperature-dependent 400 MHz ^{1}H NMR spectra of **4c** in CD_2Cl_2–$CHCl_2F$ (1:4) (174–157 K).

(rotation about C-5,N bond concerning the *Z*-s-*cis* and *E*-s-*cis* forms). In the 400 MHz spectrum of **4c** in CD_2Cl_2–$CHCl_2F$ solution (1:4) (Fig. 2), this doublet splits below 190 K into two doublets with a population ratio of 0.66:0.34 (rotation about C-4,C-5 bond).

On further cooling in CD_2Cl_2–$CHCl_2F$ below 170 K, the other signals of the s-*trans* conformer show also splittings into two signals in each case with the population ratio of 0.82:0.18

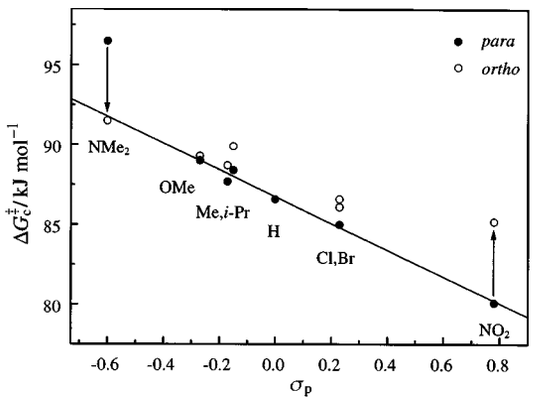

Fig. 3 Plot $\Delta G_c^{\ddagger}$ of **1** (*para*) and **3** (*ortho*) *versus* σ_p.

(rotation about C-4,C-5 bond), whereas the C-5,N rotation is not observed down to 150 K.

C-4,C-5 rotation barriers of butadienes 3

Table 3 contains the data for the C-4,C-5 rotation barriers of the *ortho*-phenyl substituted bis(methylthio)butadienes **3** compared to the *para*-substituted compounds **1**. With enhanced donor strength of X the barrier to rotation is increased in both the compounds **1** and **3**. In general, an increase of the rotation barrier of about 1 kJ mol^{-1} was found for the *ortho*-compounds. Significant deviations of $\Delta\Delta G_c^{\ddagger}$ values are observed for the dimethylamino compound **3a** and the nitro compound **3g** (Fig. 3). The strong increase of the rotation barrier of **3g** suggests a twisting of the *ortho*-nitro group out of the plane of the phenyl ring. This leads to a decrease in its electron withdrawing ability and stabilizes the ground state by increasing the C-4,C-5 double-bond character and gives an increase of the rotation barrier.

The same orthogonal arrangement of the dimethylamino group to the phenyl ring in **3a** should decrease its donor strength and, therefore, give a lower rotation barrier as is observed (Table 4). However, the large $\Delta\Delta G_c^{\ddagger}$ value for **3a** is mainly caused by the fact that the $\Delta G_c^{\ddagger}$ value for **1a** is found at about 5 kJ mol^{-1} above the regression line *versus* σ_p (Fig. 3). The reason for this is that free activation enthalpies are compared at different temperatures ($\Delta G_c^{\ddagger}$) without consideration of $\Delta S^{\ddagger} \neq 0$. The dual-parameter analysis[24] with σ_I[25] and σ_R^0[26] gave for the *para*-substituted compounds **1b**–**h** (**1a** is not included) a regression coefficient $r = 0.991$. In the case of *ortho*-substituted compounds **3**, there is a correlation with σ_I and σ_R^0 only by considering the steric interactions including the van der Waals radii r_V.[27] The maximal regression coefficient ($r = 0.987$) is found when **3a** is taken into consideration, but **3g** is not included. In this case, eqn. (1) is the linear parameter equation for **3a**–**f**,**h**.

$$\Delta G_c^{\ddagger}\ (\text{kJ mol}^{-1}) = 83.81 - 7.74\,\sigma_I - 8.69\,\sigma_R^0 + 2.30\,r_v \quad (r = 0.987) \quad (1)$$

C-3,C-4, C-4,C-5, and C-5,N rotation barriers of butadienes 4

For the aminobutadienes **4**, the rotations about C-3,C-4, C-4, C-5 and C-5,N bonds could be observed and the energy barriers were compared to those of the *para*-substituted compounds **2**[1] (Table 4).

The first $\Delta G_c^{\ddagger}$ value of the C-3,C-4 rotation in Table 4 refers to the process s-*trans*→s-*cis* and the second one to the process s-*cis*→s-*trans*. The naming of the conformers was made according to Scheme 4. As can be seen from Table 4, compared with **2**, the rotation barriers of the *ortho*-compounds **4** are increased for the first process (s-*trans*→s-*cis*) by about 2–3 kJ mol^{-1}, whereas the barriers are unchanged for the second process (s-*cis*→s-*trans*). The dimethylamino compound, **4a**,

Table 5 Selected crystal structure data of the butadienes **1a**, **3a** and **4a**

	1a	**3a**	**4a**
Sum formula	$C_{16}H_{17}N_3S_2$	$C_{16}H_{17}N_3S_2$	$C_{17}H_{20}N_4S$
M_w	315.45	315.45	312.43
Crystal size/mm	0.72 × 0.36 × 0.04	0.72 × 0.54 × 0.32	0.88 × 0.36 × 0.28
Crystal system	triclinic	triclinic	monoclinic
Space group	$P\bar{1}$	$P\bar{1}$	$P2_1/n$
a, b, c/Å	9.704(1), 10.037(1), 10.113(1)	8.236(1), 8.276(1), 12.357(1)	8.189(2), 7.648(2), 27.343(6)
α, β, γ/°	69.13(1), 78.60(1), 65.57(1)	99.48(1), 92.14(1), 98.31(1)	90.00, 93.23, 90.00
V/Å^3	836.50(15)	820.4(2)	1709.8(7)
Z	2	2	4
D_c/g cm^{-3}	1.252	1.277	1.214
Abs. coefficient μ/mm^{-1}	0.315	0.321	0.191
$F(000)$	332	332	664
2θ Range/°	4.32–44.00	5.00–43.96	5.12–44.00
h, k, l Ranges	−10/1, −10/9, −10/10	−1/9, −9/9, −13/13	−1/9, −8/1, −30/30
Reflections total	2040	2009	2079
Reflections obsd. (>2$\sigma(I)$)	1517	1725	1748
Parameters refined	194	194	204
Final R (all, obsd.)	0.0743, 0.0505	0.0469, 0.0395	0.0531, 0.0441
Final wR (all, obsd.)	0.1343, 0.1201	0.1119, 0.1014	0.1200, 0.1117

and the nitro compound, **4g**, deviate from this behavior. A similar argument as described above for **3a** and **3g** explains their anomalous $\Delta\Delta G_c^{\ddagger}$ values.

The population of the s-*trans* conformer of *ortho*-substituted compounds increases unexpectedly to 90% compared to the *para*-substituted compounds which show a 70% population.[1] This is caused by stronger twisting of the phenyl ring, which lowers the stabilization of the s-*cis* conformation by conjugative interactions between the donor side and the phenyl ring.

The relationships between rotation barriers and substituent constants, already found for **3**, were also established for the C-3,C-4 rotations in the case of **4**.

The C-5,N rotation barriers could only be estimated for the s-*cis*-butadienes, but the obtained values given in Table 4 represent lower limits. Because of the population ratios, the spectra are dominated largely by the rotation about the C-3,C-4 bond, and only after decoalescence due to this process is it possible to see the splitting of the NMe_2 signals of the s-*cis* form (DNMR5[28] simulations have shown that also the CLSA rate constants were not available in acceptable error limits). For determination of $\Delta\Delta G_c^{\ddagger}$, the value for **2a** was calculated on the basis of the correlation between the C-3,C-4 and C-5,N rotation barriers.[1] This relationship found for the *para*-substituted butadienes **2** seems to exist only qualitatively in the case of *ortho*-substituted compounds.

The C-4,C-5 rotation process in **4** leads in the 300 MHz spectra down to 170 K to signal splittings for H-4 and SMe in the s-*cis* conformers. In the case of **4a**,**b** splittings are observed for the s-*trans* conformers, too, whereas the other compounds gave only signal broadening. But, as shown for **4c**, these signals are also split in CD_2Cl_2–$CHCl_2F$ at temperatures between 170–150 K. By comparison in **2**, splittings were found only for the s-*trans*-butadienes, whereas the s-*cis*-butadienes showed no splitting down to 150 K.[1] From these results, it can be concluded that the C-4,C-5 rotation barriers in the s-*cis*-butadienes are greatly increased in the case of *ortho*-substitution.

Crystal structures of the butadienes 1a, 3a and 4a

The interpretation of the rotation barriers was additionally confirmed by results of crystal structure analyses of the butadienes. In this paper the X-ray data of compounds **1a**,**3a** and **3a**,**4a** are compared. The crystal structures of **1a**, **3a**, and **4a** are given in Fig. 4, some selected data are summarized in Table 5. The comparison of **1a** and **3a** shows for **1a** smaller torsion angles of the dimethylamino group (**1a**: 4° **3a**: 32°) and of the phenyl ring (**1a**: 30° **3a**: 60°) consistent with a stronger donor effect of the amino group in **1a** than in **3a**. Therefore, the lengths of the bonds NMe_2,aryl and C-3,aryl are diminished

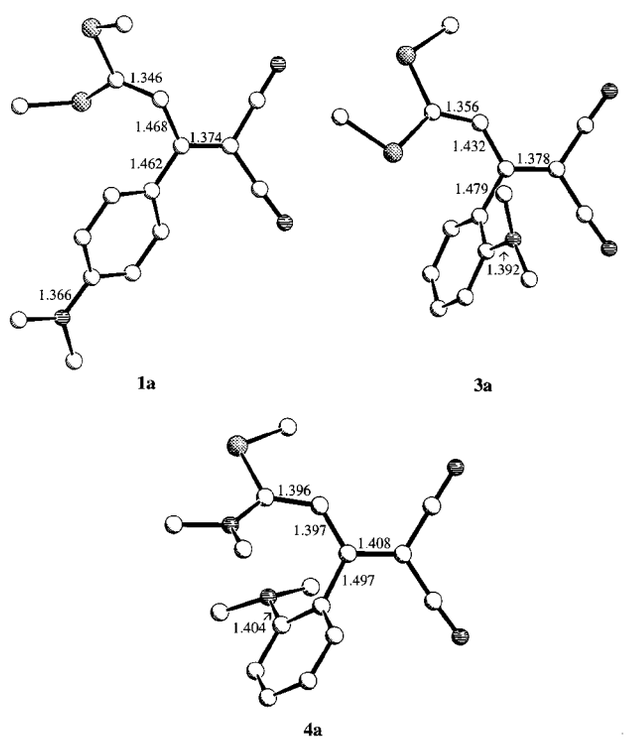

Fig. 4 Crystal structures of butadienes **1a**, **3a** and **4a** (non H atoms) with atomic distances (in Å) for selected bonds. Selected torsion angles (θ in degrees in the order of **1a**, **3a**, **4a**; calculated to $0° \le \theta \le 90°$): θ(CN(Z), C-2, C-3, C-4) = 18.2, 9.3, 10.5; θ(C-2, C-3, C-4, C-5) = 40.1, 15.5, 4.8; θ(C-3, C-4, C-5, D(Z) = 15.7, 7.3, 37.8; θ(C-2, C-3, C-1′, C-2′) = 29.9, 59.9, 57.3; θ(C-3′, C-4′, N, lone pair (**1a**); C-1′, C-2′, N, lone pair (**3a**, **4a**)) = 4.0, 31.8, 35.2.

and, simultaneously, the donor–acceptor interactions along the butadiene chain are influenced. The *para*-amino substitution increases the single-bond character of the central C-3,C-4 bond connected with a strong twisting about this bond. On the other hand, little change is observed in the C-2,C-3 and C-4,C-5 double bonds. Nevertheless, the effects are not to be neglected either. The shorter length of the C-4,C-5 bond in **1a** is in accordance with the higher rotation barriers about this bond.

The push-pull character of the compounds investigated is confirmed by comparison of the butadienes **3a** and **4a** with different donor substitution. The enhancement of the donor–acceptor interactions leads to a redistribution of the π-electron density along the butadiene chain for **4a**. In addition to the bond length changes characteristic torsion angles are found.

The torsion of the butadiene chain due to steric interactions of the aryl with the donor and acceptor side, in each case, takes place about the bonds with higher single-bond character. Accordingly, the torsion angle about the C-3,C-4 bond in **3a** is higher. On the other hand, a strong enhancement of the C-4,C-5 angle in the case of **4a** is observed (Fig. 4). In summary, the changes in bond lengths and angles are consistent with the observed rotation barriers.

Acknowledgements

The authors are grateful to B. Harzfeld for technical assistance. The Fonds der Chemischen Industrie is gratefully acknowledged for financial support.

References

1 M. Michalik, T. Freier, K. Zahn and K. Peseke, *Magn. Reson. Chem.*, 1997, **35**, 859.
2 S. Dähne, *Science*, 1978, **199**, 1163.
3 G. Ege, H. O. Frey and E. Schuck, *Synthesis*, 1979, 376.
4 M. Michalik, K. Peseke and R. Radeglia, *J. Prakt. Chem.*, 1981, **323**, 506.
5 H. Schubert, I. Bast and M. Regitz, *Synthesis*, 1983, 661.
6 M. Michalik, K. Peseke and R. Radeglia, *J. Prakt. Chem.*, 1985, **327**, 103.
7 B. S. Bogdanov, Z. A. Krasnaja and T. S. Stycenko, *Izv. Akad. Nauk SSSR, Ser. Khim.*, 1990, 1304.
8 E. P. Prokof'ev, Z. A. Krasnaja and V. F. Kucerov, *Izv. Akad. Nauk SSSR, Ser. Khim.*, 1973, 2013; *Org. Magn. Reson.*, 1974, **6**, 240.
9 M. Michalik and K. Peseke, *Z. Chem.*, 1983, **23**, 418.
10 M. Michalik, K. Zahn, P. Köckritz and J. Liebscher, *J. Prakt. Chem.*, 1989, **331**, 1.
11 (*a*) J. E. Douglas, B. S. Rabinovitch and F. S. Looney, *J. Chem. Phys.*, 1955, **23**, 315; (*b*) R. B. Cundall and T. F. Palmer, *Trans. Faraday Soc.*, 1961, **57**, 1936; (*c*) M. C. Lin and K. J. Laidler, *Can. J. Chem.*, 1968, **46**, 973.
12 M. Ōki, *Applications of Dynamic NMR Spectroscopy to Organic Chemistry*, VCH Verlagsgesellschaft, Weinheim, 1985, pp. 252.
13 K. Zahn, PhD Thesis, University of Rostock, 1991.
14 M. Michalik and K. Peseke, *Sulfur Lett.*, 1986, **5**, 55.
15 M. Michalik, Habilitationsschrift, University of Rostock, 1984.
16 P. Dastidar, T. N. Guru Row and K. Venkatesan, *Acta Crystallogr., Sect. B*, 1993, **49**, 900.
17 T. Freier, M. Michalik and K. Peseke, unpublished results.
18 A. L. van Geet, *Anal. Chem.*, 1968, **40**, 2227; *Anal. Chem.*, 1970, **42**, 679.
19 H. S. Gutowsky and G. H. Holm, *J. Chem. Phys.*, 1956, **25**, 1228.
20 H. Shanan-Atidi and K. H. Bar-Eli, *J. Phys. Chem.*, 1970, **74**, 961.
21 G. M. Sheldrick, SHELXL-93, University of Göttingen, 1993.
22 (*a*) E. Campaigne, G. F. Bulbenko, W. E. Kreighbaum and D. R. Maulding, *J. Org. Chem.*, 1962, **27**, 4428; (*b*) R. H. Prager and S. T. Were, *Aust. J. Chem.*, 1983, **36**, 1441; (*c*) W. H. N. Nijhuis, W. Verboom, A. Abu El-Fadl, S. Harkema and D. N. Reinhoudt, *J. Org.Chem.*, 1989, **54**, 199; (*d*) *Organikum*, Deutscher Verlag der Wissenschaften, Berlin, 1986, p. 460. For details, see: T. Freier, PhD Thesis, University of Rostock, 1997.
23 K. Peseke, K. Zahn and M. Michalik, *J. Prakt. Chem.*, 1994, **336**, 357.
24 C. W. Fong, S. E. Lincoln and E. H. Williams, *Aust. J. Chem.*, 1978, **31**, 2615, 2623.
25 (*a*) S. Ehrenson, R. T. C. Brownlee and R. W. Taft, *Progr. Phys. Org. Chem.*, 1973, **10**, 1; (*b*) M. Charton, *J. Org. Chem.*, 1964, **29**, 1222.
26 R. T. C. Brownlee, R. E. J. Hutchinson, A. R. Katritzky, T. T. Tidwell and R. D. Topsom, *J. Am. Chem. Soc.*, 1968, **90**, 1757.
27 (*a*) A. Bondi, *J. Phys. Chem.*, 1964, **68**, 441; (*b*) M. Charton, *J. Am. Chem. Soc.*, 1975, **97**, 1552; *J. Org. Chem.*, 1977, **42**, 2528; (*c*) G. Bott, L. D. Field and S. Sternhell, *J. Am. Chem. Soc.*, 1980, **102**, 5618.
28 D. S. Stephenson and G. Binsch, *J. Magn. Reson.*, 1978, **32**, 145; *Quant. Chem. Progr. Exch.*, 1978, **10**, 365.
29 J. Sandström, *Dynamic NMR Spectroscopy*, Academic Press, London, 1982, pp. 80.

Paper 8/05857A